Proceedings of the INMM & ESARDA Joint Virtual Annual Meeting
August 23-26 & August 30-September 1, 2021

Progress On Fission Product Yield Experiment At Oregon State University

A. S. Tamashiro
Nuclear Sci. and Eng.
Oregon State University
Corvallis, OR, USA
tamashia@oregonstate.edu

J. T. Harke
Physical Life Science
Lawrence Livermore Nat'l Lab
Livermore, CA, USA
harke2@llnl.gov

S. Burcher
Physical Life Science
Lawrence Livermore Nat'l Lab
Livermore, CA, USA
burcher1@llnl.gov

C. J. Palmer
Nuclear Sci. and Eng.
Oregon State University
Corvallis, OR, USA
camille.palmer@oregonstate.edu

S. Menn
Nuclear Sci. and Eng.
Oregon State University
Corvallis, OR, USA
scott.menn@oregonstate.edu

S. Reese
Nuclear Sci. and Eng.
Oregon State University
Corvallis, OR, USA
steve.reese@oregonstate.edu

W. Loveland
Nuclear Sci. and Eng.
Oregon State University
Corvallis, OR, USA
walter.loveland@oregonstate.edu

L. Minc
Nuclear Sci. and Eng.
Oregon State University
Corvallis, OR, USA
leah.minc@oregonstate.edu

ABSTRACT

Fission product yields play an important role for nuclear reactor fuel cycle, nuclear reactor decay heat, and nuclear reactor waste inventory. Multiple techniques have been used to determine fission product yields for many decades to support reactor design. For our purposes, we will be performing γ-ray spectroscopy on β-decaying fission products following a prompt fission neutron spectrum irradiation. Previous work has been performed using the Godiva-IV critical assembly to determine fission product yields starting 1 hour after irradiation and data was recorded for 7 days. In order to observe shorter-lived fission products, a new rabbit system and γ-ray counting setup is being developed by Lawrence Livermore National Laboratory (LLNL) and Oregon State University (OSU) for use in a campaign of measurements on ^{238}U at the OSU TRIGA reactor. The counting setup will consist of four BGO Compton-suppressed HPGe clover detectors connected to a new VME-based digital data acquisition system. Data will be recorded in list-mode to analyze time-dependant behavior of the γ-spectra. The clover detectors have relative efficiency of 150% (to 3×3 in. NaI(Tl) crystal at 1.33 MeV) and the solid angle coverage of four detectors is approximately 6% for the array. The ^{238}U samples will be delivered in front of the detectors directly from the reactor core via the rabbit facility. One complication with rabbit systems is that there may exist trace elements that will undergo neutron capture reactions and introduce extraneous γ-rays in the time scale of interest. This prompted a study of different pure polyethylene sample materials from various suppliers at the OSU TRIGA reactor and the development of a new rabbit. A preliminary

proof-of-principle measurement at the OSU TRIGA reactor will be presented along with fission products identified within 30 minutes from fission. The experimental and detection setup at LLNL will be described and future measurements will be discussed.

INTRODUCTION

Fission product yields (FPY) are relevant to nuclear fission theory, nuclear reactor design, reactor antineutrino anomaly, stellar nucleosynthesis, and nuclear forensics. Yet, the last fission product yields evaluation occurred in 1993 [1]. Since then, there have been significant improvements in detection capabilities and data processing. In collaboration with Lawrence Livermore National Laboratory (LLNL), this experiment seeks to apply state-of-the-art detectors and electronics with modifications to the existing rabbit system at the Oregon State University (OSU) Training, Research, Isotopes, General Atomics (TRIGA) reactor. The rabbit system will enable short exposure of samples and transportation to the detection setup, allowing γ-rays to be observed 3 seconds to 1 hour after irradiation. The detection system will be four Compton suppressed large high purity germanium (HPGe) detectors segmented for γ-γ coincidence and fission product yield measurements. Modern electronics will record data in list mode, bringing flexibility to the data analysis. Post processing software will be developed using ROOT [2]; a data analysis framework designed for high energy particle physics. The results will be implemented into the new Generalized Nuclear Database Structure (GNDS) format [3].

This conference proceedings will present the progress of the experimental setup and software development. A proof-of-principle measurement was performed in 2019 [4] and that data was analyzed to identify a few of the short-lived fission product yields within 30 minutes from fission.

BACKGROUND ON FISSION PRODUCT YIELD EVALUATIONS

Since the discovery of fission in 1938, there have been numerous fission product yield measurements. Around 1973, there have been multiple evaluations of fission product yields for specific applications [5]–[7]. The 1974 US evaluation [8] and the 1977 UK evaluation [9] became the basis for the comprehensive UK and US fission yield libraries. In 1976, the Chinese group initiated their fission product yield evaluation [1]. Japan and Russia were improving their own database as well [10]. International fission product yield meetings in 1987 [11] and 1989 [12] led to the International Atomic Energy Agency (IAEA) Co-ordinated Research Project (CRP). The CRP compilation and evaluation fission product yields started in 1991 and concluded with the most recent fission product yield evaluation of 1993 [1].

Currently, ENDF/B-VIII.0 uses evaluated fission product yields from the 1993 England and Rider evaluation [13]. There are 1,953 fission product yield results used for fission neutron ^{238}U cumulative fast fission product yields. The evaluators combined results from previous benchmark values, mass spectrometry, radiochemistry, gas counting, special techniques, and estimations. Radiochemistry included solely γ-ray spectroscopy measurements. There were 75 publications that are categorized as radiochemistry and 18 of these were purely γ-ray spectroscopy without any chemical separations. Two-hundred fission product yield results from 18 different measurements used γ-ray spectroscopy only. There are 53 fission products measured with half-lives ranging from 32 seconds to 285 days. Three of these measurements were performed using mono-energetic neutrons which do not equate to fission neutrons (0–10 MeV [14]). There were two measurements using NaI which do not have the energy resolution as germanium detectors for isotope identification. The most recent measurement was performed in 1988 (33 years ago from today). Overall, the measured fission product yields vary

with each other and are combined as a single evaluated value. This variance is also observed in a recent fission product yield measurement using Godiva-IV critical assembly [15]. 117 γ-rays were analyzed from 29 different isotopes. There were variations in fission product yield determined using different γ-rays from the same isotope. With comparison of past fission product yield measurements, it was concluded that the main cause of variation is the γ-ray branching ratios.

Approximately every decade, an evaluation is performed for a particular mass chain. Within a mass chain evaluation are nuclear structure evaluations for each isobar. Each nuclear structure evaluation includes a nucleus level scheme with decay branching ratios feeding into each level. Within the nuclear levels are probabilities for each internal transition (initial to final state of the nucleus). A procedure manual is provided by the Evaluated Nuclear Structure Data File (ENSDF) to perform a mass chain evaluation [16]. Part of the calculations performed by evaluators is to determine γ-ray branching ratios for specific parent decay. γ-ray branching ratios must include an internal conversion coefficient to become total intensity. Theoretical internal conversion coefficients can be calculated using the BrIcc code provided by the National Nuclear Data Center (NNDC) [17]. A program called GABS is provided by NNDC and used for normalizing total intensities to 100 decays of the parent nucleus [18]. For the case of fission product yields, the γ-rays observed are a result of a parent nucleus β-decaying and populating a daughter nucleus state.

An experiment is being designed at OSU to accomplish both fission product yield and fission product γ-ray branching ratio measurements. A highly segmented, high efficient, and high energy resolution γ-ray spectrometer setup coupled with the rapid transport of samples with the rabbit facility is being designed . The future experimental setup and electronics will be discussed in the next section.

FUTURE EXPERIMENTAL SETUP

The OSU TRIGA rabbit system allows for the transportation of samples (via rabbit tubes see Figure 1) into the reactor and back to a counting setup (see Subfigure 3f). Multiple samples of ^{238}U will be irradiated to build the counting statistics necessary in evaluating fission product yields and γ-ray branching ratios. The proposed measurement will use 12 samples of ^{238}U, but if that is not sufficient, the experiment will be repeatable to irradiate more samples.

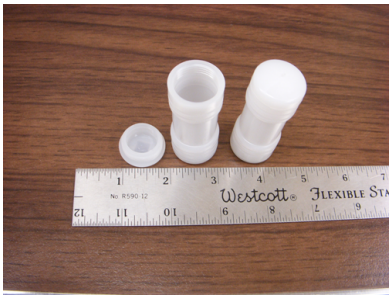

Figure 1: Sample carriers also known as rabbits.

A preliminary irradiation of the rabbit tubes showed a presence of trace elements that undergo neutron capture reactions. For an example, ^{28}Si(n,p)^{28}Al will result in a 1.78 MeV γ-ray ($\tau_{1/2} = 2.245 \pm 0.002$ m [19]). In order to reduce or eliminate as much contaminants as possible, a new rabbit is being designed with a purer polyethylene. A few companies were reached out to irradiate polyethylene samples in the OSU TRIGA reactor. The results are shown in Table 1. WestLake

Table 1: Neutron activation analysis of different polyethylene samples irradiated in the OSU TRIGA reactor.

Production Mechanism	γ-ray Energy (keV)	Specific Activity (Bq/g)		
		Westec	Shieldwerx	WestLake
	75.5	68.60	88.03	–
$^{54}\mathrm{Fe}(n,\alpha)^{51}\mathrm{Cr}\xrightarrow{\varepsilon}{}^{51}\mathrm{V}$	320.28	8.03	–	–
$^{127}\mathrm{I}(n,\gamma)^{128}\mathrm{I}\xrightarrow{\beta^-}{}^{128}\mathrm{Xe}$	442.90	8.05	–	–
e^-+e^+	511.0	476.22	135.43	8.72
$^{65}\mathrm{Cu}(n,\gamma)^{66}\mathrm{Cu}\xrightarrow{\beta^-}{}^{66}\mathrm{Zn}$	832.86	7.61	32.18	–
$^{26}\mathrm{Mg}(n,\gamma)^{27}\mathrm{Mg}\xrightarrow{\beta^-}{}^{27}\mathrm{Al}$	843.8	3.78	–	–
$^{65}\mathrm{Cu}(n,\gamma)^{66}\mathrm{Cu}\xrightarrow{\beta^-}{}^{66}\mathrm{Zn}$	1038.85	240.74	1059.14	1.67
$^{30}\mathrm{Si}(n,\gamma)^{31}\mathrm{Si}\xrightarrow{\beta^-}{}^{31}\mathrm{P}$	1267.68	2.73	–	–
$^{40}\mathrm{Ar}(n,\gamma)^{41}\mathrm{Ar}\xrightarrow{\beta^-}{}^{41}\mathrm{K}$	1293.43	302.22	975.05	3.00
$^{63}\mathrm{Cu}(n,\gamma)^{64}\mathrm{Cu}\xrightarrow{\varepsilon}{}^{64}\mathrm{Ni}$	1345.83	–	2.93	–
$^{37}\mathrm{Cl}(n,\gamma)^{38}\mathrm{Cl}\xrightarrow{\beta^-}{}^{38}\mathrm{Ar}$	1642.63	11.08	1.46	–
$^{28}\mathrm{Si}(n,p)^{28}\mathrm{Al}\xrightarrow{\beta^-}{}^{28}\mathrm{Si}$	1778.80	90.34	108.59	0.91
3084.42 keV Double Escape Peak	2062.34	0.43	–	–
$^{37}\mathrm{Cl}(n,\gamma)^{38}\mathrm{Cl}\xrightarrow{\beta^-}{}^{38}\mathrm{Ar}$	2167.22	12.08	0.97	–
3084.42 keV Single Escape Peak	2572.95	0.46	–	–
$^{48}\mathrm{Ca}(n,\gamma)^{49}\mathrm{Ca}\xrightarrow{\beta^-}{}^{49}\mathrm{Sc}$	3084.42	1.56	–	–

supplied a polyethylene much purer than the other two samples tested so far. Xometry is the company chosen to produce these rabbit tubes with WestLake's polyethylene. The redesigned rabbits will transfer the sample from the counting room, in/out of the reactor, and in front of the detection system.

There will be four clovers and four bismuth germanate ($Bi_4Ge_3O_{12}$ or abbreviated BGO) detectors (see Subfigure 3e) used to perform γ-γ coincidence measurement [20]. The clovers are detectors with 4 HPGe crystals that are named leaves. In essence, there are four leaves in each clover. Each clover can handle up to 10,000 Hz of data which is limited by the dead time. Each leaf crystal is 5cm x 5cm x 8cm and 4 leaves together makes the active area of each clover 10cm x 10cm x 8cm. A common HPGe crystal would be equivalent to 1 leaf. The BGOs are scintillation detectors that operate with a higher efficiency than the clovers. These are built to surround the clovers to be used for Compton suppression. Each BGO detector houses 16 BGO crystals to 16 photomultiplier tubes (PMT). All the data will be recorded in full and the Compton suppression will be performed in the post processing data analysis.

The front of each clover/BGO pair is a tungsten collimator, iron plate, and Teflon™ (see Figure 2). The heavy met tungsten will shield γ-rays from the source directly to the BGO. Besides background, all signals from the BGOs will be Compton scattered photons from the clovers. The Teflon™ and iron are used to shield β particles and their Bremsstrahlung X-rays respectively.

The counting setup is located in the same room as the OSU TRIGA reactor. There are background radiation produced by the reactor visible to γ-ray detectors. To reduce background photopeaks, shielding material is placed around the detection setup. Figure 3 is the lead castle assembled for

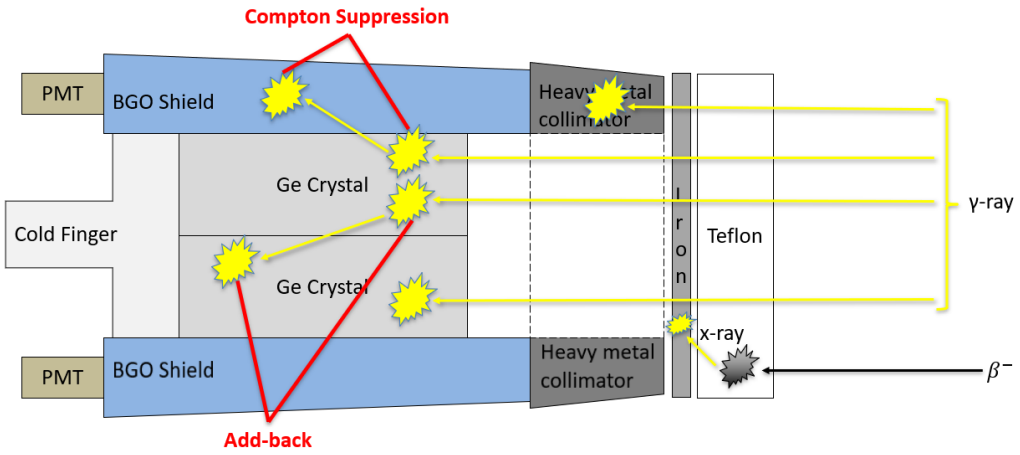

Figure 2: A cross sectional view of the front face of each clover/BGO pair.

the experiment. The shielding and detectors are held by multiple 80/20 tables.

There are 4 tables assembled with 3"x3" 80/20 pieces and 1/4" aluminum table tops. The main table is 96"x48" (see Subfigure 3b). This holds the 4 clover/BGO pairs and the lead castle. Underneath the main table is the 40"x36" bottom table (see Subfigure 3a). This holds 1 layer of lead bricks providing 2" of shielding underneath the detectors. On top of the main table are two 36"x18" tables (see Subfigure 3c). The detectors are encased by the top tables which forms the skeleton of the lead castle. The lead castle will provide at least 4" of lead shielding surrounding the detection setup (see Subfigure 3d).

In January 2020, the table and lead castle have been assembled in the reactor bay. There have been multiple testing of the lead castle showing the presence of ^{41}Ar. A HPGe detector was used at different locations to locate the source of ^{41}Ar (see Figure 4). The ^{41}Ar is located in a pipe on the side of the reactor and on the floor. The lead bricks used were standard 2"x4"x8". The 2 inches of lead is not enough to shield the ^{41}Ar 1.29 MeV γ-ray. Another layer of lead bricks on the top of the lead castle is easy, but below is challenging. Concrete blocks will be made to fit under the table to provide the additional shielding below the detectors. Also, additional lead bricks will be necessary on the reactor side of the table.

Each clovers output four signals and each BGO output one signal (sum of 16 PMT signals). The 20 total signal cables are connected into three Mesytec MDPP-16 high resolution time and amplitude digitizer [21]. An external clock is used to ensure that the time stamp does not drift by the internal clock of the system. An optical sensor in the rabbit system will provide the reset signal to align all the data in time for each ^{238}U sample irradiation. The Mesytec modules are directly mounted into a VMEbus controlled by the Mesytec MVLC VME controller [22]. The MVLC communicates with a nearby computer via Ethernet cable. A local DHCP server is set up to assign the MVLC with an IP address. The data acquisition software for this experiment is also provided by Mesytec, called MVME [23]. The data acquisition electronics will be placed into a nearby counting room and not exposed to the radiation present in the reactor bay. All raw data will be recorded into list-mode and feed into the data analysis software being developed.

DATA ANALYSIS

The raw data is decompressed using a C/C++ code, then the parsed data in ASCII text or ROOT file is imported into data analysis codes written in C/C++/ROOT. Essentially, these codes perform

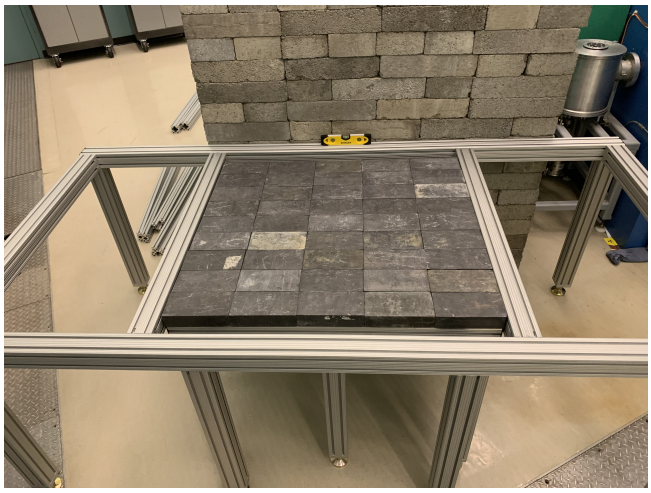

(a) Bottom table with lead bricks

(b) Main table

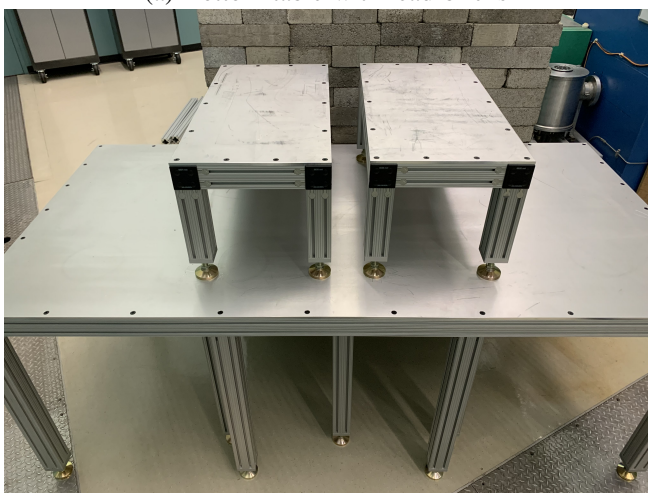

(c) Top tables

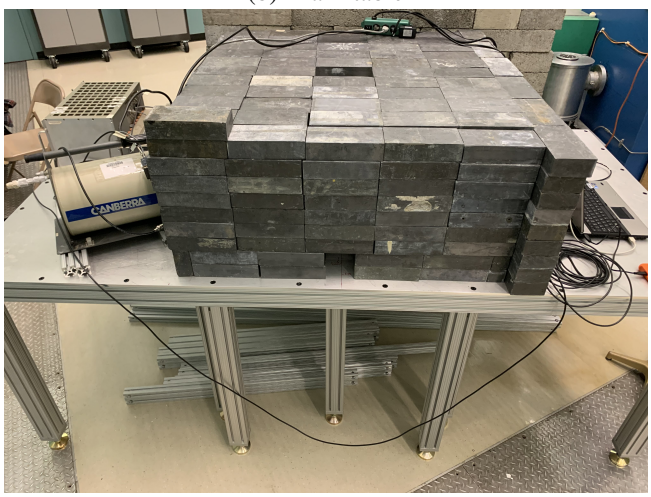

(d) Lead castle

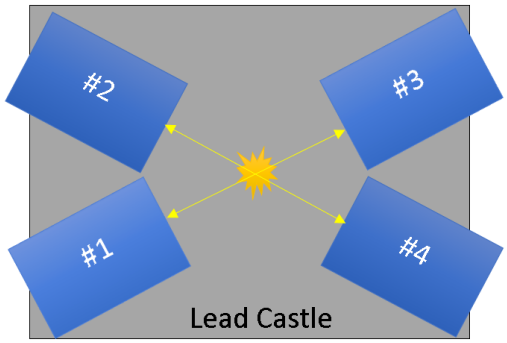

(e) Detector positioning

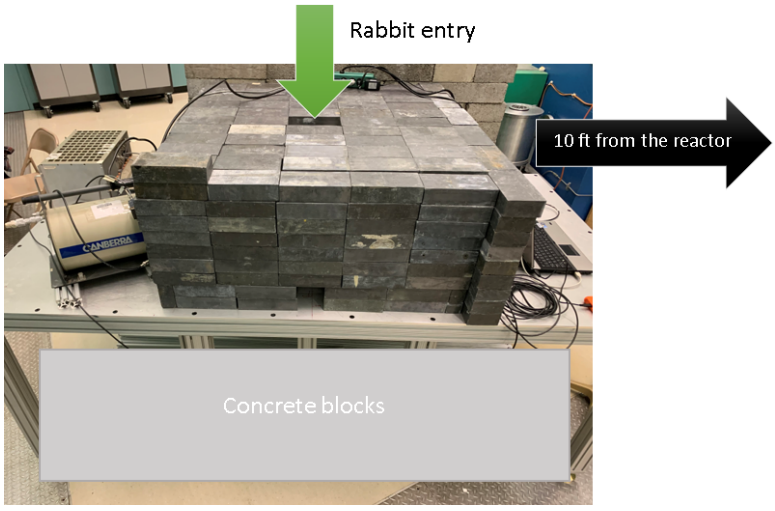

(f) Planned setup

Figure 3: Table setup located in the OSU TRIGA reactor bay.

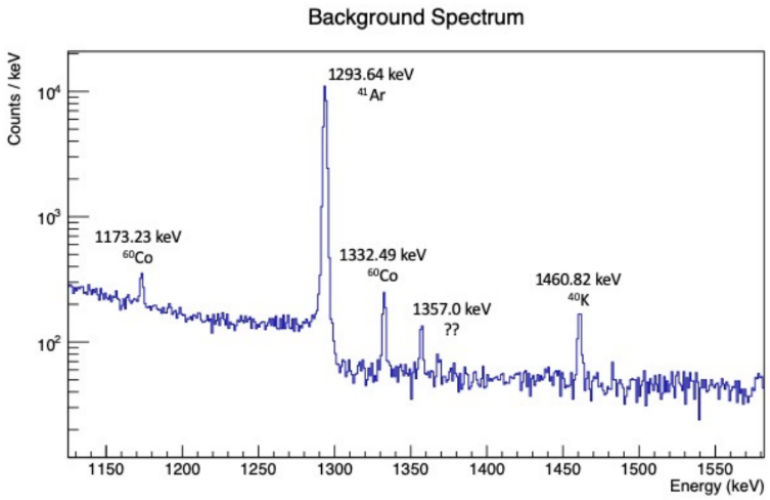

Figure 4: A background spectrum in the OSU TRIGA reactor bay.

γ-ray spectroscopy to extract the initial activity to calculate fission product yields and extract γ-γ coincidence to calculate γ-ray branching ratios.

Standard γ-ray calibration sources (see Table 2) will be used to characterize the detectors. Energy calibration, energy resolution, and detector efficiency ϵ_γ are measured. Energy calibration and resolution are used for an automated peak search algorithm being developed.

Once peak locations are identified, the net counts of the photopeaks are plotted against time to

Table 2: Radionuclides and activities that will be used for characterizing the detectors.

Standard sources	Calibration Activity (kBq)
^{22}Na	8/1/2019, 41.8 ± 1.3
^{60}Co	8/1/2019, 44.4 ± 1.3
^{133}Ba	8/1/2019, 42.0 ± 1.3
^{137}Cs	8/1/2019, 41.4 ± 1.2
^{152}Eu	8/1/2019, 43.9 ± 1.3
^{210}Pb	8/1/2019, 230 ± 6.9
^{226}Ra	8/1/2019, 28.5 ± 0.9

analyze the half-life of the γ-ray being analyzed. The decay scheme will have rapidly changing components (feed and decay). In order to successfully fit the time dependent data, a generalized Bateman equation with multiple feed and decay branches will be used as the fit function. The equation is based on the solution provided here [24]. Using a decay chain fit will result in independent initial activities to be extracted, while the highest order parent will have its cumulative initial activity extracted. The initial activities A_0 will be used for calculating fission product yields for isotope i in Equation 1.

$$FPY_i = \frac{A_{0,i}\tau_{1/2,i}}{\ln(2)N_f\epsilon_{\gamma,i}I_iR_i} \tag{1}$$

$\tau_{1/2}$ is the half-life from the fit, N_f is total fission, I is self attenuation, and R is γ-ray branching ratio. Since the samples of ^{238}U will be "thin", self attenuation is expected to be negligible, but will be measured. The branching ratio term can be replaced with the newly measured branching ratios from the γ-γ coincidence analysis.

In order to perform any sort of coincidence analysis, timing resolution must be measured. This is done by measuring the two contra-directional 511 keV γ-rays produced by the ^{22}Na positron-electron annihilation reaction. The relative γ-ray branching ratios are calculated and the GABS software can be used to convert relative γ-ray branching ratios into the γ-ray branching ratios needed for Equation 1.

PRELIMINARY RESULTS

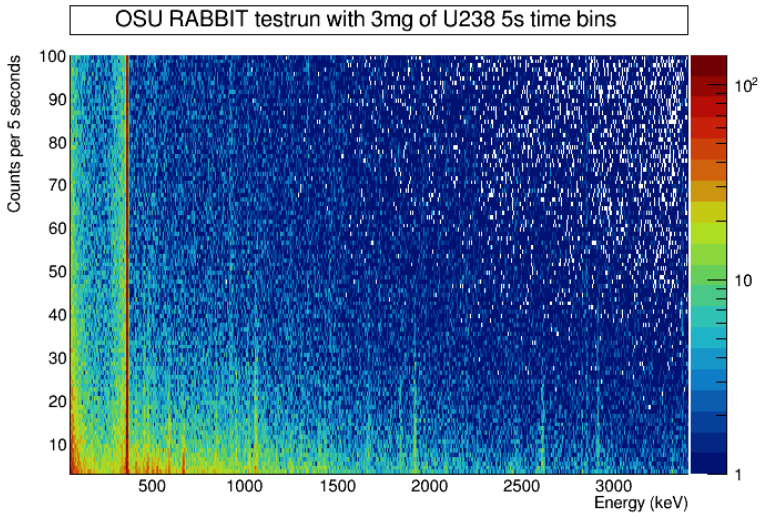

Figure 5: Five second parsed data for 3 mg of ^{238}U irradiated in the OSU TRIGA reactor for two seconds.

A test run with ^{238}U was conducted with promising results (see Figure 5). This was performed using the original rabbit tubes, but the inner encapsulation was taken out and placed in front of a HPGe detector. The data was parsed into 30 second time bins. Various γ-ray peaks were fitted using a Gaussian and linear background. The time dependent data were fitted with a decay curve to fit the half-life and identify the isotope. Table 3 lists the isotopes and their half-lives identified from the test run data. The shortest-lived fission product identified was ^{89}Rb ($\tau_{1/2} = 15.32 \pm 0.10$ minutes). The actual experiment will include twelve ^{238}U samples and using clover detectors will increase the γ-ray counting statistics by a factor of 240 (assuming one 30% HPGe detector to four 150% HPGe detectors efficiency and one to twelve samples). Besides fission, ^{238}U has a probability to undergo neutron capture, which results in populating ^{239}U ($\tau_{1/2} = 23.45 \pm 0.02$ m [25]). The rabbit facility makes it possible to measure short-lived isotopes.

CONCLUSION

The experiment is being assembled and the data analysis codes are under development. The data acquisition system is still being tested to fine tune the settings for the detection system. This work will resolve some of the discrepancies in γ-ray branching ratios and measure short-lived fission product yields with half-lives on the magnitude of seconds. The OSU experimental setup is not limited to only fission product yield studies, but can also accommodate neutron activation analysis.

Table 3: Isotopes identified from the OSU test experiment.

Isotope	Reference Half-life (hr)	Reference FPY (%) [13]
^{83}Se	0.3708 ± 0.0007 [26]	0.15 ± 0.05
^{84}Br	0.529 ± 0.001 [27]	0.82 ± 0.02
^{88}Kr	2.825 ± 0.019 [28]	2.03 ± 0.06
^{89}Rb	0.2553 ± 0.0017 [29]	2.76 ± 0.06
^{91}Sr	9.65 ± 0.06 [30]	4.04 ± 0.08
^{94}Y	0.312 ± 0.002 [31]	4.6 ± 0.2
^{105}Ru	4.439 ± 0.011 [32]	4.1 ± 0.1
^{127}Sn	2.10 ± 0.04 [33]	0.10 ± 0.05
^{128}Sn	0.985 ± 0.002 [34]	1.7 ± 1.1
^{129}Sb	4.366 ± 0.026 [35]	1.0 ± 0.2
^{130}Sb	0.66 ± 0.01 [36]	0.9 ± 0.6
^{131}Sb	0.3838 ± 0.0007 [37]	3.3 ± 0.1
^{134}Te	0.70 ± 0.01 [38]	6.8 ± 0.2
^{141}Ba	0.305 ± 0.001 [39]	5.3 ± 0.3
^{142}La	1.518 ± 0.008 [40]	4.59 ± 0.09
^{149}Nd	1.728 ± 0.001 [41]	1.63 ± 0.07
^{239}U	0.3908 ± 0.0003 [25]	–

ACKNOWLEDGEMENTS

This work was funded by the Office of Defense Nuclear Nonproliferation Research and Development within the U.S. DOE - NNSA. This work was performed under the auspices of the U.S. DOE by LLNL under Contract DE-AC52-07NA27344. This work was performed with the assistance of the Radiation Center at Oregon State University.

REFERENCES

[1] J. England and B. Rider, "Endf/b-6 fpy: The endf/b-6 fission-product yield sub-libraries," IAEA-NDS-106, Tech. Rep., 1995. [Online]. Available: https://inis.iaea.org/collection/NCLCollectionStore/_Public/32/004/32004855.pdf?r=1&r=1

[2] R. Brun and F. Rademakers, "Root—an object oriented data analysis framework," *Nuclear Instruments and Methods in Physics Research Section A: Accelerators, Spectrometers, Detectors and Associated Equipment*, vol. 389, no. 1-2, pp. 81–86, 1997.

[3] C. Mattoon, B. Beck, N. Patel, N. Summers, G. Hedstrom, and D. Brown, "Generalized nuclear data: A new structure (with supporting infrastructure) for handling nuclear data," *Nuclear Data Sheets*, vol. 113, no. 12, pp. 3145–3171, 2012, special Issue on Nuclear Reaction Data. [Online]. Available: https://www.sciencedirect.com/science/article/pii/S0090375212000944

[4] J. T. Burke, A. S. Tamashiro, B. S. Alan, S. Padgett, S. Menn, S. Reese, W. Loveland, L. Minc, C. Palmer, and K. Roberts, "Results from oregon state university 1 mw triga reactor irradiation of uranium-238," 9 2019. [Online]. Available: https://www.osti.gov/biblio/1562381

[5] E. Crouch, "Fission-product chain yields from experiments in thermal reactors," in *Nuclear data in science and technology*, 1973.

[6] W. Walker, "Cumulative yields of thermal neutron fission products: Some results and recommendations based on a recent evaluation," in *Nuclear data in science and technology*, 1973.

[7] M. Lammer and O. J. Eder, "Discussion of fission-product yield evaluation methods and a new evaluation," in *Nuclear data in science and technology*, 1973.

[8] M. E. Meek and B. F. Rider, "Compilation of fission product yields, vallecitos nuclear center, 1974," 1 1974.

[9] E. Crouch, "Fission-product yields from neutron-induced fission," *Atomic Data and Nuclear Data Tables*, vol. 19, no. 5, pp. 417 – 532, 1977. [Online]. Available: http://www.sciencedirect.com/science/article/pii/0092640X77900237

[10] R. Mills, "Thesis," 1995.

[11] M. Lammer, "Summary report of a specialists" meeting on fission yield evaluation, studsvik, sweden, 11-15 september 1987," 1988. [Online]. Available: https://www-nds.iaea.org/publications/indc/indc-nds-0208/

[12] M Lammer, "Summary report of the iaea consultants - meeting on compilation and evaluation of fission yield nuclear data, vienna, 27-29 september 1989," 1991. [Online]. Available: https://www-nds.iaea.org/publications/indc/indc-nds-0261/

[13] D. Brown *et al.*, "Endf/b-viii.0: The 8th major release of the nuclear reaction data library with cielo-project cross sections, new standards and thermal scattering data," *Nuclear Data Sheets*, vol. 148, pp. 1 – 142, 2018, special Issue on Nuclear Reaction Data. [Online]. Available: http://www.sciencedirect.com/science/article/pii/S0090375218300206

[14] R. L. Murray and K. E. Holbert, "Chapter 6 - fission," in *Nuclear Energy (Eighth Edition)*, eighth edition ed., R. L. Murray and K. E. Holbert, Eds. Butterworth-Heinemann, 2020, pp. 101 – 114. [Online]. Available: http://www.sciencedirect.com/science/article/pii/B978012812881700006X

[15] A. S. Tamashiro, "Evaluation of ^{235}u and ^{238}u fast fission product yields from godiva-iv burst irradiation via gamma detection," Jan 2019. [Online]. Available: https://ir.library.oregonstate.edu/concern/graduate_thesis_or_dissertations/sb397f11f

[16] M. R. Bhat, "Procedures manual for the evaluated nuclear structure data file," 10 1987.

[17] T. Kibédi, T. Burrows, M. Trzhaskovskaya, P. Davidson, and C. Nestor, "Evaluation of theoretical conversion coefficients using bricc," *Nuclear Instruments and Methods in Physics Research Section A: Accelerators, Spectrometers, Detectors and Associated Equipment*, vol. 589, no. 2, pp. 202 – 229, 2008. [Online]. Available: http://www.sciencedirect.com/science/article/pii/S0168900208002520

[18] J. K. Tuli, "Evaluated nuclear structure data file–a manual for preparation of data sets." Brookhaven National Lab., Upton, NY (US), Tech. Rep., 2001.

[19] M. Shamsuzzoha Basunia, "Nuclear data sheets for a = 28," *Nuclear Data Sheets*, vol. 114, no. 10, pp. 1189–1291, 2013. [Online]. Available: https://www.sciencedirect.com/science/article/pii/S0090375213000653

[20] R. Hughes, J. Burke, R. Casperson, S. Ota, S. Fisher, J. Parker, C. Beausang, M. Dag, P. Humby, J. Koglin, E. McCleskey, A. McIntosh, A. Saastamoinen, A. Tamashiro, E. Wilson, and T. Wu, "The hyperion particle-γ detector array," *Nuclear Instruments and Methods in Physics Research Section A: Accelerators, Spectrometers, Detectors and Associated Equipment*, vol. 856, pp. 47 – 52, 2017. [Online]. Available: http://www.sciencedirect.com/science/article/pii/S0168900217303376

[21] Mesytec, "Mdpp-16." [Online]. Available: https://www.mesytec.com/products/nuclear-physics/MDPP-16.html

[22] ——, "Mvlc." [Online]. Available: https://www.mesytec.com/products/nuclear-physics/MVLC.html

[23] ——, "Mvme." [Online]. Available: https://www.mesytec.com/downloads/mvme.html

[24] P. Aarnio, "Decay and transmutation of nuclides," *CERN CMS-NOTE-1998/086*, 1998.

[25] E. Browne and J. Tuli, "Nuclear data sheets for a = 239," *Nuclear Data Sheets*, vol. 122, pp. 293–376, 2014. [Online]. Available: https://www.sciencedirect.com/science/article/pii/S0090375214006693

[26] E. McCutchan, "Nuclear data sheets for a = 83," *Nuclear Data Sheets*, vol. 125, pp. 201–394, 2015. [Online]. Available: https://www.sciencedirect.com/science/article/pii/S0090375215000034

[27] D. Abriola, M. Bostan, S. Erturk, M. Fadil, M. Galan, S. Juutinen, T. Kibédi, F. Kondev, A. Luca, A. Negret, N. Nica, B. Pfeiffer, B. Singh, A. Sonzogni, J. Timar, J. Tuli, T. Venkova, and K. Zuber, "Nuclear data sheets for a = 84," *Nuclear Data Sheets*, vol. 110, no. 11, pp. 2815–2944, 2009. [Online]. Available: https://www.sciencedirect.com/science/article/pii/S0090375209000891

[28] E. McCutchan and A. Sonzogni, "Nuclear data sheets for a = 88," *Nuclear Data Sheets*, vol. 115, pp. 135–304, 2014. [Online]. Available: https://www.sciencedirect.com/science/article/pii/S009037521300094X

[29] B. Singh, "Nuclear data sheets for a = 89," *Nuclear Data Sheets*, vol. 114, no. 1, pp. 1–208, 2013. [Online]. Available: https://www.sciencedirect.com/science/article/pii/S0090375213000021

[30] C. M. Baglin, "Nuclear data sheets for a = 91," *Nuclear Data Sheets*, vol. 114, no. 10, pp. 1293–1495, 2013. [Online]. Available: https://www.sciencedirect.com/science/article/pii/S0090375213000665

[31] D. Abriola and A. Sonzogni, "Nuclear data sheets for a = 94," *Nuclear Data Sheets*, vol. 107, no. 9, pp. 2423–2578, 2006. [Online]. Available: https://www.sciencedirect.com/science/article/pii/S0090375206000652

[32] S. Lalkovski, J. Timar, and Z. Elekes, "Nuclear data sheets for a=105," *Nuclear Data Sheets*, vol. 161-162, pp. 1–353, 2019. [Online]. Available: https://www.sciencedirect.com/science/article/pii/S0090375219300614

[33] A. Hashizume, "Nuclear data sheets for a = 127," *Nuclear Data Sheets*, vol. 112, no. 7, pp. 1647–1831, 2011. [Online]. Available: https://www.sciencedirect.com/science/article/pii/S009037521100055X

[34] Z. Elekes and J. Timar, "Nuclear data sheets for a = 128," *Nuclear Data Sheets*, vol. 129, pp. 191–436, 2015. [Online]. Available: https://www.sciencedirect.com/science/article/pii/S0090375215000472

[35] J. Timar, Z. Elekes, and B. Singh, "Nuclear data sheets for a = 129," *Nuclear Data Sheets*, vol. 121, pp. 143–394, 2014. [Online]. Available: https://www.sciencedirect.com/science/article/pii/S0090375214006565

[36] B. SINGH, "Nuclear data sheets for a = 130," *Nuclear Data Sheets*, vol. 93, no. 1, pp. 33–242, 2001. [Online]. Available: https://www.sciencedirect.com/science/article/pii/S0090375201900122

[37] Y. Khazov, I. Mitropolsky, and A. Rodionov, "Nuclear data sheets for a = 131," *Nuclear Data Sheets*, vol. 107, no. 11, pp. 2715–2930, 2006. [Online]. Available: https://www.sciencedirect.com/science/article/pii/S0090375206000809

[38] A. Sonzogni, "Nuclear data sheets for a = 134," *Nuclear Data Sheets*, vol. 103, no. 1, pp. 1–182, 2004. [Online]. Available: https://www.sciencedirect.com/science/article/pii/S0090375204000717

[39] N. Nica, "Nuclear data sheets for a = 141," *Nuclear Data Sheets*, vol. 122, pp. 1–204, 2014. [Online]. Available: https://www.sciencedirect.com/science/article/pii/S009037521400667X

[40] T. Johnson, D. Symochko, M. Fadil, and J. Tuli, "Nuclear data sheets for a = 142," *Nuclear Data Sheets*, vol. 112, no. 8, pp. 1949–2127, 2011. [Online]. Available: https://www.sciencedirect.com/science/article/pii/S0090375211000676

[41] B. Singh, "Nuclear data sheets for a=149," *Nuclear Data Sheets*, vol. 102, no. 1, pp. 1–291, 2004. [Online]. Available: https://www.sciencedirect.com/science/article/pii/S0090375204000390